RESEARCH ACTIVITIES II
Department of Molecular Structure

II-A Laser Cooling and Trapping of Metastable Helium Atoms

In the past two decades, extensive developments have occurred in the laser cooling and trapping of neutral atoms, with many workers reporting the application of these techniques to such diverse atomic species as alkali atoms, alkali earth atoms, and rare gas atoms. Among these, the helium atom is unique on account of its small mass, simple energy level structure, and easy availability in two isotopic forms (^{3}He and ^{4}He) of differing quantum statistics. For this reason, we have been studying the laser cooling and trapping of helium atoms.

II-A-1 Magneto-Optical Trap of Metastable Helium-3 Atoms

KUMAKURA, Mitsutaka; MORITA, Norio

[*Appl. Phys. B: Lasers Opt.* **70**, 555 (2000)]

A magneto-optical trap (MOT) of metastable ^{3}He atoms has been demonstrated for the first time. Some 10^5 atoms have successfully been confined in a region with a diameter of ~0.4 mm at a temperature of ~0.5 mK; the atomic number density is estimated to be ~10^9 /cm^3 at the trap center. These characteristics of the ^{3}He MOT are almost comparable to those of the ^{4}He MOT so far demonstrated by many workers. Monitoring the fluorescence from the MOT, the trap loss rate has also been measured and discussed. Since ^{3}He is a unique fermionic atom on account of its small mass and simple energy level structure, we can expect that such a ^{3}He MOT will be useful as a fundamental tool for future studies on the physics of fermions at ultralow temperatures.

II-B Spectroscopic Studies on Atoms and Ions in Liquid Helium

Atoms and ions in liquid helium are known to reside in bubble-like cavities due to the Pauli repulsive force between electrons. Physical properties of these exotic surroundings are determined by the potential energy of the impurity-He$_n$ system, the surface tension energy of the liquid helium, and the pressure-volume work. Spectroscopic studies of such impurity atoms and ions in liquid helium are expected not only to give information on the structure and dynamics of the bubbles but also to contribute to the study on the property of superfluid liquid helium.

II-B-1 Theoretical Studies on the Spectra of Yb^+ Ions in Liquid Helium

MORIWAKI, Yoshiki; MORITA, Norio

[*Eur. Phys. J. D* **13**, 11 (2001)]

In our previous experimental studies on Yb^+ in liquid helium, we found that its spectra have two characteristic properties: (1) The $4f^{14}6s^2S_{1/2}$–$6p^2P_{1/2}$ (D1) excitation spectrum is much broadened and blue-shifted compared with the spectrum of free Yb^+ ions, while the emission spectrum of the same transition has relatively small spectral width and shift compared with the excitation spectrum. (2) The excitation spectrum of the $4f^{14}6s^2S_{1/2}$–$6p^2P_{3/2}$ (D2) transition is doubly peaked. To explain these properties, we have carried out theoretical calculations on the basis of a vibrating bubble model, in which the bubble surface is assumed to vibrate in the spherical (breathing), dipolar and quadrupolar modes. These calculations are essentially based on adiabatic potential curves of an Yb^+–He pair, which have been obtained from our complete-active-space self-consistent field (CASSCF) and multi-reference configuration-interaction (MRCI) calculations. Consequently, it has been found that the blue shifts are well understood with this bubble model, and also that the dynamic Jahn-Teller effect due to the quadrupole vibration of the bubble plays an important role for the double-peaked profile of the D2 excitation spectrum.

II-B-2 Measurements of Fine Structure Changing Cross Sections of Ca^+ and Sr^+ in Collisions with He Atoms

MORIWAKI, Yoshiki; MATSUO, Yukari[1]; MORITA, Norio
([1]RIKEN)

In our previous spectroscopic study of Yb^+ in liquid helium, we observed an emission from its $4f^{14}6p\ ^2P_{1/2}$ fine structure level not only when this level was directly excited but also when another fine structure level ($4f^{14}6p\ ^2P_{3/2}$) was excited. This suggested the presence of a fast inter-multiplet transition from $^2P_{3/2}$ to $^2P_{1/2}$ due to the interaction between Yb^+ and He atoms. From our estimation, which was based on the comparison between the emission intensities measured when the $^2P_{1/2}$ and $^2P_{3/2}$ levels were excited, we found that the $^2P_{3/2} \rightarrow {}^2P_{1/2}$ transition should be extremely faster than expected

for two-body collisions of other atoms and ions with He. This enhancement of the transition may have arisen from some many-body effect, such as the quadrupole vibration of the helium bubble surface. However we could not discuss it any more, because there were no data on the fine structure changing rate in two-body collisions, which was necessary to exactly estimate the many-body effect. This fact motivated us to study fine structure changing rates of alkali-earth ions in two-body collisions with He.

We have started with measurements on Ca^+ and Sr^+ to test our experimental apparatus. These ions have been produced by laser ablation of pure metal samples. Detecting laser induced fluorescence, we have measured cross sections of collision induced transitions between fine structure levels in the $4p^2P_J$ state of Ca^+ and the $5p^2P_J$ state of Sr^+ due to collisions with He atoms at room temperature (298 K). The cross sections obtained are $\sigma(Ca^+: 4p^2P_{3/2} \rightarrow 4p^2P_{1/2}) = 1.17 \pm 0.05$ Å^2, $\sigma(Ca^+: 4p^2P_{1/2} \rightarrow 4p^2P_{3/2}) = (7.92 \pm 0.44) \times 10^{-1}$ Å^2, and $\sigma(Sr^+: 5p^2P_{3/2} \rightarrow 5p^2P_{1/2}) = (1.44 \pm 0.10) \times 10^{-2}$ Å^2. These cross sections are much smaller than those of neutral K and Rb atoms, which have the same electron configurations as Ca^+ and Sr^+, respectively. This may probably be because stronger spin-orbit couplings in the $2P_J$ states of Ca^+ and Sr^+ prevent their electron spins from flip-flopping all the more. On the other hand, it is known that the cross sections of alkali atoms are roughly proportional to $e^{-C\Delta E}$ (where ΔE is the fine structure splitting and C is a constant). This is seen from the fact that the cross sections for alkali atoms are almost on a straight line in Figure 1. However, the present cross sections for Ca^+ and Sr^+ significantly deviate upward from this line, as seen in Figure 1; that is, these cross sections are much larger than expected from only the sizes of the fine structure splittings. This may probably be due to a difference between the interactions in ion-He and atom-He pairs.

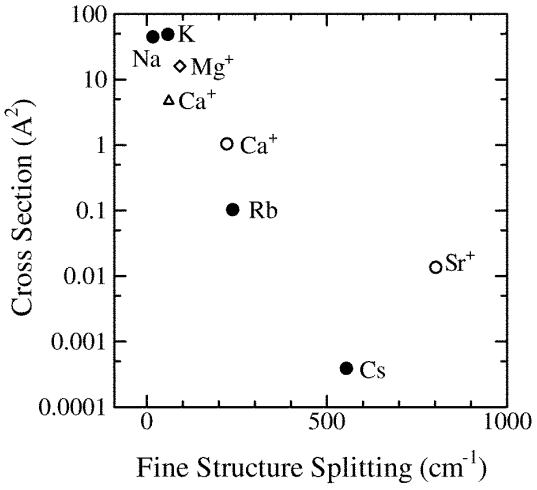

Figure 1. Fine structure changing cross sections so far measured for various alkali atoms and alkali earth ions in collisions with He atoms, as a function of their fine structure splittings; ● shows the one for the $np^2P_{3/2} \rightarrow np^2P_{1/2}$ transition of each alkali atom (for Na, K, Rb and Cs, n = 3, 4, 5 and 6, respectively, and the collision temperature T = 397, 368, 340 and 311 K, respectively) (by Krause), ◇ Mg^+ $3p^2P_{3/2} \rightarrow 3p^2P_{1/2}$ at 1600 K (by Brust), △ Ca^+ $3d^2D_{5/2} \rightarrow 3d^2D_{3/2}$ at 10000 K (by Knoop *et al.*), and ○ the present data.

II-C Endohedral Metallofullerenes: New Fullerene Molecules with Novel Properties

Encapsulation of one or more metal atoms inside hollow fullerene cages (endohedral metallofullerenes) has long attracted special attention because it could lead to new sperical molecules with novel properties unexpected for empty fullerenes. Great efforts have been made for the production and characterization of endohedral metallofullerenes. Up to now it has been demonstrated that group 2 and 3 metals and most lanthanide metals can be trapped inside the higher fullerenes to form soluble and relatively stable endohedral metallofullerenes. Because of the difficulty in producing pure samples in large quantities, the experimental characterization of endohedral metallofullerenes has been hindered. Recent important progress is marked by the successful isolation and purification of metallofullerenes in macroscopic quantities. This has made it possible to investigate the interesting electronic properties and chemical reactivities.

II-C-1 La@C_{82} Anion. An Usually Stable Metallofullerene

AKASAKA, Takeshi[1]; WAKAHARA, Takatsugu[2]; NAGASE, Shigeru[3]; KOBAYASHI, Kaoru[3]; WÄLCHLI, Markus[4]; YAMAMOTO, Kazunori[5]; KONDO, Masahiro[2]; SHIRAKURA, Shingo[2]; OKUBO, Shingo[2]; MAEDA, Yutaka[2]; KATO, Tatsuhisa; KAKO, Masahiro[6]; NAKADAIRA, Yasuhiro[6]; NAGAHATA, Ritsuko[7]; GAO, Xiang[8]; VAN CAEMELBECKE, Eric[8]; KADISH, Karl M.[8]
([1]IMS and Niigata Univ.; [2]Niigata Univ.; [3]Tokyo Metropolitan Univ.; [4]Bruker Japan; [5]PRN; [6]Univ. Electro-Commun.; [7]NIMCR; [8]Univ. Houston)

[*J. Am. Chem. Soc.* **122**, 9316 (2000)]

The anion of the major isomer of La@C_{82} was electrochemically prepared and isolated. Anionic La@C_{82}(–) is very stable in water, even after exposure to air at room temperature. The high stability of La@C_{82}(–) is essentially due to its closed-shell electronic structure. As evidenced by the ESR analysis, La@C_{82}(–) is diamagnetic. These experimental findings are confirmed by density functional calculations. The cage structure of La@C_{82} was determined for the first time and shown to have C_{2v} symmetry based on the ^{13}C NMR measurements of the compound in its anionic form.

II-C-2 Transient Spectroscopic Properties of Endohedral Metallofullerenes, La@C_{82} and La_2@C_{80}

FUJITSUKA, Mamoru[1]; ITO, Osamu[1]; KOBAYASHI, Kaoru[2]; NAGASE, Shigeru[2]; YAMAMOTO, Kazunori[3]; KATO, Tatsuhisa; WAKAHARA, Takatsugu[4]; AKASAKA, Takeshi[5]
([1]Tohoku Univ.; [2]Tokyo Metropolitan Univ.; [3]PRN; [4]Niigata Univ.; [5]IMS and Niigata Univ.)

[*Chem. Lett.* 902 (2000)]

Properties of the excited states of endohedral metallofullerenes (La@C_{82} and La_2@C_{80}) have been investigated by time-resolved absorption spectroscopy. Transient absorption bands of La@C_{82} showed two decay-components, which were attributed to excited states of different spin multiplicity. The properties of photoexcited states of La_2@C_{80} are also reported.

II-C-3 Vibrational Spectroscopy of Endohedral Dimetallofullerene, La_2@C_{80}

MORIYAMA, Masaya[1]; SATO, Tadatake[1]; YABE, Akira[1]; YAMAMOTO, Kazunori[2]; KOBAYASHI, Kaoru[3]; NAGASE, Shigeru[3]; WAKAHARA, Takatsugu[4]; AKASAKA, Takeshi[5]
([1]NIMCR.; [2]PRN; [3]Tokyo Metropolitan Univ.; [4]Niigata Univ.; [5]IMS and Niigata Univ.)

[*Chem. Lett.* 524 (2000)]

The first FT-IR spectra of La_2@C_{80} are observed at temperatures from 353 to 83 K by dispersing the sample into the KBr pellet, which confirm that the C_{80} cage has I_h symmetry, as supported from theoretical calculations. Also discussed is the rotational motion of the C_{80} cage.

II-D Structure and Function of Respiratory Terminal Oxidases

In the aerobic respiratory chain of *Escherichia coli*, there are structurally unrelated two terminal oxidases. A heme-copper oxidase, cytochrome *bo* is predominantly expressed under highly aerated growth conditions while an alternative oxidase, a putative heme-heme oxidase, cytochrome *bd*, is predominant under microaerobic conditions. Both oxidases catalyze the two-electron reduction of ubiquinol-8 and the four-electron reduction of dioxygen, whereas only cytochrome *bo* exhibits vectorial proton transport. However, only a little structural information has been given for these ubiquinol oxidases. To clarify the molecular mechanism of electron transfer, chemical reaction of dioxygen, and proton pumping in the two respiratory terminal oxidases, we utilize various molecular spectroscopic techniques (*e.g.*, resonance Raman, EPR, FTIR) in conjunction with methods of molecular biology and biochemistry.

II-D-1 Probing Molecular Structure of Dioxygen Reduction Site of Bacterial Quinol Oxidases through Ligand Binding to the Redox Metal Centers

TSUBAKI, Motonari[1,2]; HORI, Hiroshi[2]; MOGI, Tatsushi[3]
([1]Himeji Inst. Tech.; [2]Osaka Univ.; [3]Univ. Tokyo)

[*J. Inorg. Biochem.* **82**, 19 (2000)]

Cytochromes *bo* and *bd* are structurally unrelated terminal ubiquinol oxidases in the aerobic respiratory chain of *Escherichia coli*. The high-spin heme-Cu_B binuclear center serves as the dioxygen reduction site for cytochrome *bo*, and the heme b_{595}-heme *d* binuclear center for cytochrome *bd*. Cu_B coordinates three histidine ligands and serves as a transient ligand binding site en route to high-spin heme, one-electron donor to the oxy intermediate, and a binding site for bridging ligands like cyanide. In addition, it can protect the dioxygen reduction site through binding of a peroxide ion in the resting state, and connects directly or indirectly Tyr288 and Glu286 to carry out redox-driven proton pumping in the catalytic cycle. Contrary, heme b_{595} of cytochrome *bd* participate a similar role to Cu_B in ligand binding and dioxygen reduction but cannot perform such versatile roles because of its rigid structure.

II-D-2 Active Site Structure of SoxB-Type Cytochrome bo_3 Oxidase from Thermophilic *Bacillus*

UCHIDA, Takeshi[1]; TSUBAKI, Motonari[1,2,4]; KUROKAWA, Tatsunori[3]; HORI, Hiroshi[4]; SAKAMOTO, Junshi[3]; KITAGAWA, Teizo[1]; SONE, Nobuhito[3]
([1]IMS; [2]Himeji Inst. Tech.; [3]Kyushu Inst. Tech.; [4]Osaka Univ.)

[*J. Inorg. Biochem.* **82**, 65 (2000)]

Two-subunit SoxB-type cytochrome *c* oxidase in *Bacillus stearothermophilus* was over-produced, purified, and examined for its active site structures by electron paramagnetic resonance (EPR) and resonance Raman (RR) spectroscopies. This is cytochrome bo_3 oxidase contained heme B at the low-spin heme site and heme O at the high-spin heme site of the binuclear center. EPR spectra of the enzyme in the oxidized form indicated that structures of the high-spin heme O and the low-spin heme B were similar to those of SoxM-type oxidases based on the signals at g = 6.1, and g = 3.04. However, the EPR signals from the Cu_A center and the integer spin system at the binuclear center showed slight differences. RR spectra of the oxidized form showed that heme O was in a 6-coordinated high-spin (ν_3 = 1472 cm^{-1}), and heme B was in a 6-coordinated low-spin (ν_3 = 1500 cm^{-1}) state. The Fe^{2+}–His stretching mode was observed at 211 cm^{-1}, indicating that the Fe^{2+}–His bond strength is not so much different from those of SoxM-type oxidases. On the contrary, both the Fe^{2+}–CO stretching and Fe^{2+}–C–O bending modes differed distinctly from those of SoxM-type enzymes, suggesting some differences in the coordination geometry and the protein structure in the proximity of bound CO in cytochrome bo_3 from those of SoxM-type enzymes.

II-E Structure and Function of Transmembrane Electron Transfer System in Neuroendocrine Secretory Vesicles

In neuroendocrine secretory vesicles of animals, intravesiclular ascorbate (AsA^-) functions as the electron donor for copper-containing monooxygenases. Upon these monooxygenase reactions, monodehydroascorbate (MDA) radical is produced by oxidation of AsA^-. The MDA radical is reduced back to AsA^- by membrane-spanning cytochrome b_{561}. Subsequently, the oxidized cytochrome b_{561} is reduced by cytosolic AsA^-. We found previously that purified cytochrome b_{561} from bovine adrenal medulla contains two hemes B per molecule, each exhibiting an independent EPR signal in oxidized state. Radiolytically generated MDA radical oxidized rapidly reduced cytochrome b_{561} to yield the oxidized form. Subsequently, the oxidized form was re-reduced by AsA^- in the medium. At excess MDA radical, only half of the heme was oxidized, indicating that only one of the two heme

centers can react with MDA radical.

II-E-1 Reduction of Heme Iron Suppresses the Carbethoxylation of Two Histidyl and One Tyrosyl Residues Indispensable for the Transmembrane Electron Transfer Reaction of Cytochrome b_{561}

TAKEUCHI, Fusako[1]; KOBAYASHI, Kazuo[2]; TAGAWA, Seiichi[2]; TSUBAKI, Motonari[1,3]
([1]Himeji Inst. Tech.; [2]Osaka Univ.; [3]IMS)

We found previously that treatment of oxidized cytochrome b_{561} with diethyl pyrocarbonate (DEPC) caused specific *N*-carbethoxylation of three fully conserved residues (His88, His161, and Lys85) located at the extravesicular side.[1)] The modification lead to a selective loss of the electron accepting ability from AsA^- without affecting the electron-donation to MDA radical. In the present study, we found that the *O*-carbethoxylation of one tyrosyl residue (Tyr218) locating at the extravesicular side was significantly enhanced in an alkaline condition, leading to a very slow reduction process of the oxidized heme with AsA^-. Presence of AsA^- during the reaction with DEPC was found to suppress the carbethoxylation of the heme-coordinating histidyl (His88 and His161) and the tyrosyl (Tyr218) residues, whereas the modification level of Lys85 was not affected. Concomitantly, the final reduction level of heme *b* with AsA^- was protected, although the fast reduction process was not fully restored. A similar protective effect was observed in the presence of sodium dithionite or isoascorbate. These results suggest that the modification of the histidine residues were suppressed in the reduced form of heme *b*. On the other hand, Tyr218, together with Lys85, has a role in the recognition/binding process for AsA^- and is indispensable for the fast electron transfer reaction from AsA^-.

Reference

1) Tsubaki, M., Kobayashi, K., Ichise, T., Takeuchi, F. and Tagawa, S., *Biochemistry* **39**, 3276 (2000).

II-E-2 Planarian Cytochrome b_{561}: A Transmembrane Electron Transfer Protein Unique to Neuroendocrine Secretory Vesicles

ASADA, Akikazu[1]; KUSAKAWA, Takashi[1]; ORII, Hidefumi[1]; AGATA, Kiyokazu[1]; WATANABE, Kenji[1]; TSUBAKI, Motonari[1,2,3]
([1]Himeji Inst. Tech.; [2]IMS; [3]Osaka Univ.)

Cytochrome b_{561} is a major transmembrane protein of catecholamine and neuropeptide secretory vesicles of central and peripheral nervous system in higher animals. We succeeded in the cloning of a full-length cDNA encoding planarian cytochrome b_{561}. The deduced amino acid sequence showed a very similar transmembrane topology to those of higher vertebrate and contained both putative AsA^-- and MDA radical-binding sites.[1)] Among the six totally-conserved His residues in higher vertebrate, one His residue was substituted with Asn residue indicating that His88 and His161 of bovine cytochrome b_{561} play roles as the heme *b* ligands at the extravesicular side. Northern- and Western-blot analyses confirmed the expression of the mRNA and the protein in planarian with the expected sizes, respectively. Distributions of the mRNA and the apoprotein were analyzed with in situ hybridization and immunocytochemical staining, respectively, which showed two morphologically distinct structures, a pair of the ventral nerve cords and the cephalic ganglion cluster in the head region. Present results suggest that the usage of AsA^- for the supply of electron equivalents to the neuroendocrine-specific copper-containing monooxygenases could be originated from organisms having a very simple nervous system.

Reference

1) Okuyama, E., Yamamoto, R., Ichikawa, Y. and Tsubaki, M., *Biochim. Biophys. Acta* **1383**, 269 (1998).

II-F Structure and Function of Steroidogenic Cytochrome P450 System

In adrenal cortex of higher animals, various cytochromes P450 perform steroid hormone biosynthesis. In the mitochondrial inner membranes, cytochromes P450scc and P45011β receive electron equivalents from a 2Fe-2S type ferredoxin, adrenodoxin, to perform the oxygen activation and the site-specific hydroxylations. On the other hand, in the endoplasmic reticulum membranes, there are two microsomal type cytochromes P450; namely P450c21 and P45017α. These cytochromes receive electron equivalents from flavin-containing cytochrome P450 reductase. The former catalyzes the C21 hydroxylation essential for the production of corticosteroid hormones (glucocorticoids and mineralcorticoids). We are currently investigating these steroidogenic cytochrome P450 systems utilizing various biochemical and biophysical techniques.

II-F-1 Direct Heme-Steroid Interaction in Cytochrome P450c21 Studied by FTIR Spectroscopy

TSUBAKI, Motonari[1,2]; TAKEUCHI, Kohji[1]
([1]Himeji Inst. Tech.; [2]IMS)

We showed previously that combination of 20β-hydroxysteroids (17α,20β-dihydroxyprogesterone and 20β-hydroxyprogesterone) with oxidized cytochrome P450c21 purified from bovine adrenocortical microsomes induced a type I difference spectrum and exhibited a concomitant development of a new low-spin

signal at g_z = 2.42, g_y = 2.21, and g_x = 1.966 and an increase in intensity of the *g*8 high-spin signal in EPR spectra.[1)] Being consistent with these substrate-like properties, we confirmed that cytochrome P450c21 have a 20β-oxidase activity for the 20β-hydroxysteroids in an enzyme-reconstituted system. In the present study, the heme-steroid interaction in reduced state was investigated by analyzing heme-bound C–O stretching vibration with FTIR spectroscopy, to clarify the mechanism of the site- and stereo-selective 20β-oxidase activity. In a substrate-free state, a C–O band was observed at 1949 cm^{-1}. Addition of 17α-hydroxyprogesterone or progesterone caused a peak-shift to 1952 and 1942.5 cm^{-1}, respectively. Additions of 17α,20β-dihydroxyprogesterone and 20β-hydroxyprogesterone caused a shift of main band to 1950 and 1955 cm^{-1}, respectively. Concomitantly, peculiar C–O bands were observed around 1998 cm^{-1} for these 20β-hydroxysteroid complexes. These results suggest a specific interaction between steroid hydroxy group(s) and heme prosthetic group, both in oxidized and reduced states.[2)]

References

1) Tsubaki, M., Matsumoto, N., Tomita, S., Ichikawa, Y. and Hori, H., *Biochim. Biophys. Acta* **1390**, 197 (1998).
2) Tsubaki, M., in *Molecular Steroidogenesis*, M. Okamaoto, Y. Ishimura and H. Nawata, Eds., Universal Academy Press, Inc.; Tokyo, pp. 69–72 (2000).

II-F-2 Adrenodoxin-Cytochrome P450scc Interaction as Revealed by EPR Spectroscopy: Comparison with Putidaredoxin-Cytochrome P450cam System

TAKEUCHI, Kohji[1]; TSUBAKI, Motonari[1,2,3]; HORI, Hiroshi[3]
([1]Himeji inst. Tech.; [2]IMS; [3]Osaka Univ.)

Cholesterol side-chain cleavage reaction catalyzed by cytochrome P450scc constitutes of three consecutive monooxygenase reactions (22R-hydroxylation, 20S-hydroxylation, and C20-C22 bond scission) to produce pregnenolone.[1,2)] The electron equivalents necessary for the oxygen activation were supplied from a 2Fe2S-type ferredoxin, adrenodoxin. We found that binding of oxidized adrenodoxin to ferric P450scc complexed with cholesterol or 25-hydroxycholesterol caused a shift of the g = 8 and g = 3.5 high-spin signal of the heme moiety but not for the low-spin signals at 15 K. On the other hand, ligation of CO or NO to the ferrous heme of P450scc complexed with reduced adrenodoxin and various steroid substrates did not show any change in a trough (at 346.8 mT) of the axial EPR spectrum of the reduced adrenodoxin (at 77 K). These results showed a remarkable contrast to those found for the cytochrome P450cam-putidaredoxin-substrate ternary complex suggesting that mode of the cross talk between adrenodoxin and P450scc is different from the *Pseudomonas system*.

References

1) Tsubaki, M., Hiwatashi, A., Ichikawa, Y. and Hori, H., *Biochemistry* **26**, 4527 (1987).
2) Tsubaki, M., Iwamoto, Y., Hiwatashi, A. and Ichikawa, Y., *Biochemistry* **28**, 6899 (1989).

II-G Biomolecular Science

Elucidation of a structure-function relationship of metalloproteins is a current subject of this group and for this purpose we treat proteins and model compounds of their active sites. The primary technique used for this project is the stationary and time-resolved resonance Raman spectroscopy excited by visible and UV lasers. The main themes that we want to explore are (1) mechanism of oxygen activation by enzymes, (2) mechanism of active proton translocation and its coupling with electron transfer, (3) coupling mechanism of proton- and electron transfers by quinones in photosynthetic reaction center, (4) higher order protein structures and their dynamics, and (5) reactions of biological NO. In category (1), we have examined a variety of terminal oxidases, cytochrome P450s, and peroxidases, and also treated their enzymatic reaction intermediates by using the mixed flow transient Raman apparatus and the Raman/absorption simultaneous measurement device. For (2) the third generation UV resonance Raman (UVRR) spectrometer was constructed and we are going to use it to the peroxy and ferryl intermediates of cytochrome *c* oxidase and cytochrome *bo*. In (3) we succeeded in observing RR spectra of quinones A and B in bacterial photosynthetic reaction centers for the first time, but we have focused our attention on detecting tyrosine radical for the P intermediate of terminal oxidases. Some positive evidence was obtained for cytochrome *bo*. For (4) we developed a novel technique for UV resonance Raman measurements based on the combination of the first/second order dispersions of gratings and applied it successfully to 235-nm excited RR spectra of several proteins including mutant hemoglobins and myoglobins. Nowadays we can carry out time-resolved UVRR experiments with nanosecond resolution to discuss protein dynamics. With the newly developed third generation UV Raman spectrometer, we have succeeded in isolating the spectrum of tyrosinate in ferric Hb M Iwate, which was protonated in the ferrous state, and that of the deprotonated state of Tyr244 of bovine cytochrome *c* oxidase. For (5) we purified soluble guanylate cyclase from bovine lung and observed its RR spectra. To further investigate it, we are developing an expression system of this protein.

II-G-1 Resonance Raman Investigation of Fe–N–O Structure of Nitrosylheme in Myoglobin and Its Mutants

TOMITA, Takeshi[1]; HIROTA, Shun[2]; OGURA, Takashi[3]; OLSON, John S.[4]; KITAGAWA, Teizo
([1]Tohoku Univ.; [2]Nagoya Univ.; [3]Univ. Tokyo; [4]Rice Univ.)

[*J. Phys. Chem. B* **103**, 7044 (1999)]

Resonance Raman spectra have been observed for NO adducts of wild-type (WT) sperm whale myoglobin (MbNO) and its H64G, H64L, L29W, V68W, and V68T mutants at neutral and acidic pH. Raman excitation in resonance with the Soret band enabled us to detect the Fe–NO stretching ($\nu_{Fe–NO}$), N–O stretching (ν_{NO}), and Fe–N–O bending (δ_{FeNO}) bands. The $\nu_{Fe–NO}$, δ_{FeNO}, and ν_{NO} bands of WT MbNO at neutral pH were observed at 560, 452, and 1613 cm^{-1}, respectively, and substitution of the distal His64 to Gly or Leu caused an upshift of ν_{NO} to 1631–1635 cm^{-1} but no change in $\nu_{Fe–NO}$. This change in ν_{NO} is considered to be due to the removal of hydrogen bonding between His64 and bound NO. Conversely, substitution of Leu29 with tryptophan (L29W) altered Fe–NO but caused no change in ν_{NO} at neutral pH. This feature resembles that of MbO_2 but distinctly differs from that of MbCO, for which the Fe–CO and C–O stretching frequencies have an inverse linear correlation. The change in $\nu_{Fe–NO}$ for L29W-MbNO is probably caused by tilting of the Fe–N bond from the heme normal on account of steric hindrance from the large indole ring but would not be due to changes in the Fe–N–O bond angle. When pH is lowered to 4, MbNO adopts the five-coordinate structure due to cleavage of the Fe-His bond. Accordingly, the heme maker bands such as ν_3 and ν_{10}, shifted from 1500 and 1636 cm^{-1} at pH 7.4 to 1509 and 1646 cm^{-1} at pH 4 which are in agreement with those of a five-coordinate Fe-protoporphyrin-NO complex in detergent micelles at neutral pH. The $\nu_{Fe–NO}$ and ν_{NO} bands of acidic MbNO were observed at 520 and 1668 cm^{-1} and exhibited no shift when the distal His was replaced by Gly or Leu. The latter observation supports previous X-ray crystallographic, infrared, and resonance Raman studies which show that the distal histidine becomes protonated at pH 4 and swings out into the solvent away from the bound ligand.

II-G-2 Novel Iron Porphyrin-Alkanethiolate Complex with Intramolecular NH···S Hydrogen Bond: Synthesis, Spectroscopy, and Reactivity

SUZUKI, Noriyuki[1]; HIGUCHI, Tunehiko[1]; URANO, Yasuteru[1]; KIKUCHI, Kazuya[1]; UEKUSA, Hidehiro[2]; OHASHI, Yuji[2]; UCHIDA, Takeshi; KITAGAWA, Teizo; NAGANO, Tetsuo[1]
([1]Univ. Tokyo; [2]Tokyo Inst. Tech.)

[*J. Am. Chem. Soc.* **121**, 11571 (1999)]

Among heme enzymes, cytochrome P450 and NO synthase (NOS) have strong oxidizing ability and unusual structure, in that their heme irons have thiolate coordination. We report here a novel iron porphyrin-alkanethiolate complex with an intramolecular NH···S hydrogen bond that we synthesized in order to examine the influence of the NH···S hydrogen bond on catalytic oxidation. Complex 1 (see Figure 1) was designed to form an NH···S hydrogen bond by introducing amide NH in the vicinity of the thiolate, while complexes 2 and 3 were designed not to form an NH···S hydrogen bond by replacing amide NH with N-methyl or by introducing acetamide in a position apart from the sulfur atom.

Complexes 1-3 were characterized by FAB MS, IR, EPR, electronic absorption spectroscopy, resonance Raman spectroscopy, and X-ray crystal structure

analysis. The absorption spectra of the ferrous-CO complexes of 1-3 exhibited typical hyperporphyrin spectra for a thiolate-ligated iron(II) porphyrin-CO complex. The Soret band of the ferrous-CO complex of 1 (456 nm, which arises from a transition between the lone pair p orbital of the thiolate and the e_g orbital of heme) was considerably blue-shifted compared to that of the other complexes, indicating electron deficiency of thiolate in complex 1 arising from the NH···S hydrogen bond.

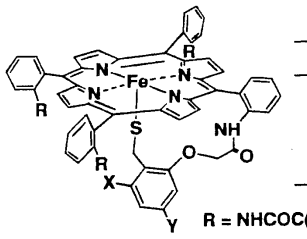

	X	Y
1	-NHCOCH$_3$	H
2	-N(CH$_3$)COCH$_3$	H
3	H	-NHCOCH$_3$
SR	H	H

Figure 1. Structures of complexes 1–3 and **SR**.

II-G-3 Mechanism of the Anionic Cyclopolymerization of Bis(dimethylvinylsilyl)methane

SUGA, Yasuhiro[1]; OKU, Jun-ichi[1]; MASUDA, Hideki[1]; TAKAKI, Mikio[1]; MUKAI, Masahiro[2]; KITAGAWA, Teizo
([1]Nagoya Inst. Tech.; [2]RIKEN)

[*Macromolecules* **32**, 1362 (1999)]

The driving force of the complete cyclization in the anionic cyclopolymerization of bis(dimethylvinylsilyl)-methane with *n*-BuLi/TMEDA in hexane is clarified with resonance Raman and ^{1}H NMR measurements. Vinyl groups coordinating to the lithium cation are detected in both measurements of the polymerization mixture at –70 °C, and they, at least some part of them, are shown to be the vinyl groups in uncyclized end units. Disappearance of these species from the resonance Raman spectrum at –20 °C indicates that the cyclization proceeds fast and is accelerated by the coordination of the second vinyl group in the uncyclized end unit. This is the first case that the interaction between the vinyl group in an uncyclized end unit and the counterion was found in ionic cyclopolymenzation.

II-G-4 Synthesis and Characterization of Novel Alkylperoxo Mononuclear Iron(III) Complexes with a Tripod: Pyridylamine Ligand: A Model for Peroxo Intermediates in Reactions Catalyzed by Non-Heme Iron Enzymes

WADA, Akira[1]; OGO, Seiji; WATANABE, Yoshihito; MUKAI, Masahiro[2]; KITAGAWA, Teizo; JUTSUKAWA, Koichiro[1]; MASUDA, Hideki[1]; EINAGA, Hisahiko[1]
([1]Nagoya Inst. Tech.; [2]RIKEN)

[*Inorg. Chem.* **38**, 3592 (1999)]

Previously, by the use of a tripodal pyridylamine ligand, tris-(6-neopentylanaino-2-pyridylmethyl)amine (TNPA), we first succeeded in the preparation of [Fe(tnpa)(OH)(PhCOO)]ClO_4 as a model complex for an active form of soybean lipoxygenase-1, in which stable formation of the hydroxo-iron(III) complex was accomplished by intramolecular hydrogen bonds. We also achieved the isolation of [Cu(bppa)(OOH)]ClO_4 having Cu(II)-OOH species by employing a similar tripodal pyridylamine ligand, bis(6-pivalamido-2-pyridylmethyl)(2-pyridylmethyl)amine (BP-PA). Here, in order to understand the coordination environment of peroxo intermediates in reactions catalyzed by non-heme iron enzymes, we have tried to synthesize stable alkylperoxo mono-nuclear iron(III) complexes using BPPA ligand and to examaine the physicochemical properties.

The resonance Raman spectra of a MeCN solution containing the complex **2** which were measured at room temperature by using 600 nm laser excitation revealed strong resonance-enhanced Raman features at 873, 838, 629, and 469 cm^{-1}, while that of **3** exhibited the features at 878, 838, 639, 548, and 493 cm^{-1}. The Raman features normally observed at ca. 800 cm^{-1} are in the range characteristic of ν(O–O) vibrations of peroxide species and are insensitive upon the addition of $H_2{}^{18}O$. Since these vibrational data were in agreement with those observed for the terminal η^1-alkylperoxo species obtained from the reaction of Fe(II)–(6–Me_3TPA) complexes with alkylperoxides, we deduced that the alkylperoxo moiety is retained on the iron(III) ion in an end-on fashion and the intense absorption bands near 585 and 613 nm for complexes **2** and **3**, respectively, are thus assignable to the alkylperoxo-to-iron(III) charge transfer transition.

II-G-5 Interactions of Phosphatidylinositol 3-Kinase Src Homology 3 Domain with Its Ligand Peptide Studied by Absorption, Circular Dichroism, and UV Resonance Raman Spectroscopies

OKISHIO, Nobuyuki[1]; NAGAI, Masako[1]; FUKUDA, Ryuji[1]; NAGATOMO, Shigenori; KITAGAWA, Teizo
([1]Kanazawa Univ.)

[*Biopolymers (Biospectroscopy)* **57**, 208 (2000)]

Absorption, circular dichroism (CD), and UV resonance Raman (UVRR) spectroscopies were applied to selectively examine the environmental and structural changes of Trp and Tyr residues in the phosphatidylinositol 3-kinase (PI3K) SH3 domain induced by ligand association. Comparison of the spectra of PI3K SH3 in the presence or absence of its ligand peptide RLP1 (RKLPPRPSK) indicated that RLP1 binding changed the environment of Trp55 of the SH3 to be more hydrophilic and its H bonding weaker and that of Tyr residues to be more hydrophobic. The D21N mutant (Asp21 → Asn) of the SH3 yielded a UV CD distinct from that of the wild type, and its spectral changes induced by RLP1 binding were smaller and different from those of the wild type in absorption, CD, and UVRR spectra, suggesting that the mutation of conserved Asp21 affected the conformation of the

ligand binding cleft and thus might lead to the decrease in the ligand affinity. These data provide direct evidence for the occurrence of environmental and structural changes of PI3K SH3 by the association of a ligand and the D21N mutation.

II-G-6 Resonance Raman Studies of Oxo Intermediates in the Reaction of Pulsed Cytochrome *bo* with Hydrogen Peroxide

UCHIDA, Takeshi; MOGI, Tatsushi[1]; KITAGAWA, Teizo
([1]Univ. Tokyo)

[*Biochemistry* **39**, 6669 (2000)]

Cytochrome *bo* from *Escherichia coli*, a member of the heme-copper terminal oxidase superfamily, physiologically catalyzes reduction of O_2 by quinols and simultaneously translocates protons across the cytoplasmic membrane. The reaction of its ferric pulsed form with hydrogen peroxide was investigated with steady-state resonance Raman spectroscopy using a home-made microcirculating system. Three oxygen-isotope-sensitive Raman bands were observed at 805/X, 783/753, and (767)/730 cm^{-1} for intermediates derived from $H_2{}^{16}O_2/H_2{}^{18}O_2$. The experiments using $H_2{}^{16}O^{18}O$ yielded no new bands, indicating that all the bands arose from the Fe=O stretching ($\nu_{Fe=O}$) mode. Among them, the intensity of the 805/X cm^{-1} pair increased at higher pH and the species giving rise to this band seemed to correspond to the P intermediate of bovine cytochrome *c* oxidase (CcO) on the basis of the reported fact that the P intermediate of cytochrome *bo* appeared prior to the formation of the F species at higher pH. For this intermediate a Raman band assignable to the C–O stretching mode of a tyrosyl radical was deduced at 1489 cm^{-1} from difference spectra. This suggests that the P intermediate of cytochrome *bo* contains an Fe^{IV}=O heme and a tyrosyl radical like compound I of prostaglandin H synthase. The 783/753-cm^{-1} pair, which was dominant at neutral pH and close to the $\nu_{Fe=O}$ frequency of the oxoferryl intermediate of CcO, presumably arises from the F intermediate. On the contrary, the (767)/730-cm^{-1} species has no counterpart in CcO. Its presence may support the branched reaction scheme proposed previously for O_2 reduction by cytochrome *bo*.

II-G-7 A New Measurement System for UV Resonance Raman Spectra of Large Proteins and Its Application to Cytochrome *c* Oxidase

AKI, Michihiko[1]; OGURA, Takashi[2]; SHINZAWA-ITOH, Kyoko[3]; YOSHIKAWA, Shinya[3]; KITAGAWA, Teizo
([1]GUAS; [2]Univ. Tokyo; [3]Himeji Inst. Tech.)

[*J. Phys. Chem. B* **104**, 10765 (2000)]

A new type of ultraviolet resonance Raman (UVRR) measurement system suitable to a limited amount of large protein samples is proposed and the results from its application to bovine cytochrome *c* oxidase (CcO) is presented. To minimize the sample damage caused by high-flux UV laser illumination and to reject visible fluorescence from the sample, frequency-doubling of a mode-locked Ar^+ ion laser and a solar blind multi-channel detector were employed, respectively. A new spinning cell was designed so that the sample solution could be stirred during spinning of the cell. Combination of all these devices resulted in successful observation of high quality UVRR spectra of CcO excited at 244 nm. The RR bands of tryptophan- and tyrosine residues dominated the observed spectra, while an extra band appeared at 1656 cm^{-1}. The frequency of the extra band as well as those of all other bands were unaltered by the redox change of metal centers and ligand binding to heme a_3. Deprotonation of a tyrosine residue(s) with a low pK_a value was detected for the resting state at pH 9.1. Examination of all possible assignments led us to conclude that the extra band arose from the linoleoyl side chain of phospholipids and its intensity suggested the presence of 21 linoleoyl groups per CcO molecule.

II-G-8 An Approach to the O_2 Activating Mononuclear Non-heme Fe Enzymes: Structural Characterization of Fe(II)-Acetato Complex and Formation of Alkylperoxoiron(III) Species with the Highly Hindered Hydrotris(3-tert-butyl-5-isopropyl-1-pyrazolyl)borate

OGIHARA, Tamako[1]; HIKICHI, Shiro[1]; AKITA, Munetaka[1]; UCHIDA, Takeshi; KITAGAWA, Teizo; MORO-OKA, Yoshihiko[1]
([1]Tokyo Inst. Tech.)

[*Inorg. Chim. Acta* **297**, 162 (2000)]

Structural characterization of an F(II)-acetato complex and attempts to synthesize mononuclear Fe(III) dioxygen complexes bearing the highly sterically demanding $Tp^{tBu,iPr}$ (= hydrotris(3-tert-butyl-5-isopropyl-1-pyrazolyl)borate) ligand have been investigated. X-ray crystallography reveals that the acetato complex consists of the distorted square pyramidal Fe(II) center as found for the previously reported O_2-reactive Tp^{iPr2} derivative. In contrast to the less hindered Tp^{iPr2}, (= hydrotris(3,5-diiso-propyl-1-pyrazolyl)borate) complexes, oxidative addition of O_2 to the coordinatively unsaturated Fe(II) centers of the acetato and a hydroxo complexes with $Tp^{tBu,iPr}$ has never been observed in any conditions. Reaction of the ferrous hydroxo complex with ROOH (R = H, alkyl) results in the formation of the thermally unstable intermediates. Especially, the Fe(III)-alkylperoxo complex is characterized by UV-Vis, ESR and resonance Raman spectroscopy. The extremely bulky $Tp^{tBu,iPr}$ ligand hinders the approach of the exogenous O_2 molecule to the Fe(II) centers but stabilizes the unstable Fe(III)alkylperoxo intermediate enough to be detected.

II-G-9 Structures of Reaction Intermediates of Bovine Cytochrome *c* Oxidase Probed by Time-Resolved Vibrational Spectroscopy

KITAGAWA, Teizo

[*J. Inorg. Biochem.* **82**, 9 (2000)]

Structures of reaction intermediates of bovine cytochrome *c* oxidase (CcO) in the reactions of its fully reduced form with O_2 and fully oxidized form with H_2O_2 were investigated with time-resolved resonance Raman (RR) and infrared spectroscopy. Six oxygen-associated RR bands were observed for the reaction of CcO with O_2. The isotope shifts for an asymmetrically labeled dioxygen, $^{16}O^{18}O$, has established that the primary intermediate of cytochrome a_3 is an end-on type dioxygen adduct and the subsequent intermediate (P) is an oxoiron species with Fe=O stretch ($\nu_{Fe=O}$) at 804/764 cm^{-1} for $^{16}O_2/^{18}O_2$ derivatives, although it had been long postulated to be a peroxy species. The P intermediate is converted to the F intermediate with $\nu_{Fe=O}$ at 785/751 cm^{-1} and then to a ferric hydroxy species with ν_{Fe-OH} at 450/425 cm^{-1} (443/417 cm^{-1} in D_2O). The rate of reaction from P to F intermediates is significantly slower in D_2O than in H_2O. The reaction of oxidized CcO with H_2O_2 yields the same oxygen isotope-sensitive bands as those of P and F, indicating the identity of intermediates. Time-resolved infrared spectroscopy revealed that deprotonation of carboxylic acid side chain takes place upon deligation of a ligand from heme a_3. UVRR spectrum gave a prominent band due to *cis* C=C stretch of phospholipids tightly bound to purified CcO.

II-G-10 Heme Structure of Hemoglobin M Iwate [α87(F8)His → Tyr]: A UV and Visible Resonance Raman Study

NAGAI, Masako[1]; AKI, Michihiko[2]; LI, Renqiang[1], JIN, Yayoi[1]; SAKAI, Hiroki[3]; NAGATOMO, Shigenori; KITAGAWA, Teizo
([1]Kanazawa Univ.; [2]GUAS; [3]Sakai Womens Clinic)

[*Biochemistry* **39**, 13093 (2000)]

Heme structures of a natural mutant hemoglobin (Hb), Hb M Iwate [α87(F8)His → Tyr], and protonation of its F8-Tyr were examined with the 244-nm excited UV resonance Raman (UVRR) and the 406.7- and 441.6-nm excited visible resonance Raman (RR) spectroscopy. It was clarified from the UVRR bands at 1605 and 1166 cm^{-1} characteristic of tyrosinate that the tyrosine (F8) of the abnormal subunit in Hb M Iwate adopts a deprotonated form. UV Raman bands of other Tyr residues indicated that the protein takes the T quaternary structure even in the *met*-form. Although both hemes of α and β subunits in *met*Hb A takes a six-coordinate (6c) high-spin structure, the 406.7-nm excited RR spectrum of *met*Hb M Iwate indicated that the abnormal α subunit adopts a 5c high-spin structure. The present results and our previous observation of the $\nu_{Fe-O(tyrosine)}$ Raman band (*Biochemistry* **28**, 2418, (1989)) have proved that F8-tyrosinate is covalently bound to Fe(III)-heme in the α subunit of Hb M Iwate. As a result, peripheral groups of porphyrin ring, especially the vinyl and the propionate side chains, were so strongly influenced that the RR spectrum in the low frequency region excited at 406.7 nm is distinctly changed from the normal pattern. When Hb M Iwate was fully reduced, the characteristic UVRR bands of tyrosinate disappeared and the Raman bands of tyrosine at 1620 (Y8a), 1207 (Y7a), and 1177 cm^{-1} (Y9a) increased in intensity. Coordination of distal His(E7) to the Fe(II)-heme in the reduced α subunit of Hb M Iwate was proved by the observation of the ν_{Fe-His} RR band in the 441.6-nm excited RR spectrum at the same frequency as that of its isolated α chain. The effects of the distal-His coordination on the heme appeared as distortion of the peripheral groups of heme. Possible mechanism for the formation of Fe(III)-tyrosinate bond in Hb M Iwate is discussed.

II-G-11 Model Complexes for the Active Form of Galactose Oxidase. Physicochemical Properties of Cu(II)- and Zn(II)-Phenoxyl Radical Complexes

ITOH, Shinobu[1]; TAKI, Masayasu[2]; KUMEI, Hideyuki[2]; TAKAYAMA, Shigehisa[2]; NAGATOMO, Shigenori; KITAGAWA, Teizo; SAKURADA, Norio[3]; ARAKAWA, Ryuichi[3]; FUKUZUMI, Shunichi[2]
([1]Osaka City Univ.; [2]Osaka Univ.; [3]Kansai Univ.)

[*Inorg. Chem.* **39**, 3708 (2000)]

One-electron oxidations of the Cu(II)- and Zn(II)-phenolate complexes of ligand 1H afford relatively stable phenoxyl radical complexes, which exhibit very characteristic UV-NIR features similar to those exhibited by the active forms of the native enzymes. Comparison of the spectroscopic characteristics (UV-vis and ESR) of the Cu(II) and Zn(II) complexes of $1^{\bullet}$ to those of the corresponding complexes of $2^{\bullet}$ indicates that the methylthio group of $1^{\bullet}$ exerts an electron-sharing conjugative effect, thus stabilizing the radical form of the cofactor, as has been demonstrated in model studies of the metal-free radicals. Such an important role for the thioether group (electron-sharing conjugative effect) has also been predicted by ab initio theory and demonstrated by high-frequency ESR studies of model radicals. It should be noted, however, that such an electronic effect of an alkylthio group is not always observed in other model systems, suggesting that the molecular geometry of a complex is also very important to the enhancement of this effect. The smaller ε values for the NIR features of the model complexes as compared to those for the active forms of the native enzymes may indicate a strong contribution from $Tyr272^{\bullet} \rightarrow Tyr495^{-}$ interligand charge transfer in addition to intramolecular charge transfer from the benzene ring to the alkylthio group in the phenoxyl radical group itself in the enzymatic systems.

II-G-12 Characterization of Imidazolate-Bridged Cu(II)-Zn(II) Heterodinuclear and Cu(II)-Cu(II) Homodinuclear Hydroperoxo Complexes as Reaction Intermediate Models of Cu, Zn-SOD

OHTSU, Hideki[1]; ITOH, Shinobu[2]; NAGATOMO, Shigenori; KITAGAWA, Teizo; OGO, Seiji;

WATANABE, Yoshihito; FUKUZUMI, Shunichi[1]
([1]Osaka Univ.; [2]Osaka City Univ.)

[*Chem. Commun.* 1051 (2000)]

Imidazolate-bridged Cu(II)-Zn(II) heterodinuclear and Cu(II)-Cu(II) homodinuclear hydroperoxo complexes are generated in the reactions between imidazolate-bridged heterodinuclear homodinuclear complexes and H_2O_2 in the presence of triethylamine base and characterized spectroscopically as reaction intermediate models of Cu, Zn-SOD.

II-H Fast Dynamics of Photoproducts in Solution Phases

Picosecond time-resolved resonance Raman (ps-TR^3) spectroscopy is a promising technique to investigate ultrafast structural changes of molecules. However, this technique has not been used as widely as nanosecond TR^3 spectroscopy, mainly due to the lack of light source which has suitable repetition rates of pulses and wavelength tunability. In order to obtain qualified TR^3 spectra, first we need two independently tunable light sources for pump and probe pulses. Second, the repetition rate should be higher than kilohertz to keep a moderate average laser power without making the photon density of probe pulse too high. We succeeded in developing light sources for ps-TR^3 spectroscopy having wide tunability and kHz repetition, and applied them to study fast dynamics of photo-excited molecules. For carbonmonoxy myoglobin (MbCO), vibrational relaxation with the time constant of 1.9 ps was observed for CO-photodissociated heme. For Ni-octaethylporphyrin in benzene, differeces in rise times of population in vibrationally excited levels among various modes were observed in the anti-Stokes spectra for the first time. This technique has been applied to identify the trans ligand of CO in the CO-bound transcriptional factor, Coo A.

On the other hand, we have constructed a nanosecond temperature-jump apparatus using a water absorption in near infrared. The new apparatus based on a Nd:YAG laser was combined with a time-resolved Raman measurement system and applied successfully to explore thermal unfolding of ribonuclease A.

II-H-1 Saturation Raman Spectroscopy as a tool for Studying the Excited States of Complex Organic Molecules: Application to Nickel Octaethylporphyrin

KRUGLIK, Sergei G.[1]; SHVEDKO, A. G.[1]; KITAGAWA, Teizo
([1]B. I. Stepanov Inst. Phys.)

[*Asian J. Phys.* **17**, 365 (1998)]

The nanosecond saturation resonance Raman (RR) technique has been reviewed and its peculiarities have been examined on the basis of a well-known molecular system, nickel octaethylporphyrin [Ni(OEP)] in solution. The results of mathematical treatment of saturation RR spectra of Ni(OEP) in weakly coordinating pyridine solvent suggest that the quantum yield of photogeneration of the six-coordinate Ni(OEP)-(pyridine)$_2$ species is low, with the rate of complexation process being about one tenth of the rate of excitation deactivation within the manifold of four-coordinate species.

II-H-2 Construction of Novel Nanosecond Temperature Jump Apparatuses Applicable to Raman Measurements and Direct Observation of Transient Temperature

YAMAMOTO, Kohji[1]; MIZUTANI, Yasuhisa; KITAGAWA, Teizo
([1]GUAS)

[*Appl. Spectrosc.* in press (2000)]

Two types of nanosecond temperature jump (T-jump) apparatuses applicable to time-resolved Raman measurements were constructed. T-jump was achieved by direct heating of water using near infrared (NIR) pulses at 1.89 μm in one type and at 1.56 μm in the other. The two NIR pulses were generated through stimulated Raman scattering (SRS) of H_2 or D_2 excited by the fundamental line of a Q-switched Nd:YAG laser, in which a single pass configuration with H_2 was sufficient for 1.89-μm pulses but a seeding-amplification configuration with D_2 was necessary for 1.56-μm pulses. The seeding-amplification configuration brought about significant improvements in conversion efficiency, pulse-to-pulse stability, and beam quality. These apparatuses were applied to transient Raman measurements of MoO_4^{2-} solution and transient temperatures of the heated volume were determined from ratios of anti-Stokes to Stokes Raman intensities. Temporal behaviors of the temperature of heated volume upon illumination of nanosecond heat pulses at 1.89-μm or 1.56-μm were explored and its applicability to studies on the primary process of thermal reactions was examined. It became clear that the continuation time of raised temperature is determined only by replacement of sample in the case of thick sample and by both thermal transfer and sample replacement in a case of thin sample, while thermal diffusion is not effective for both samples.

II-H-3 Identification of Histidine 77 as the Axial Heme Ligand of Carbonmonoxy CooA by Picosecond Time-Resolved Resonance Raman Spectroscopy

UCHIDA, Takeshi; ISHIKAWA, Haruto[1]; ISHIMORI, Koichiro[1]; MORISHIMA, Isao[1]; NAKAJIMA, Hiroshi[2]; AONO, Shigetoshi[2]; MIZUTANI, Yasuhisa; KITAGAWA, Teizo
([1]Kyoto Univ.; [2]JIST)

[*Biochemistry* **39**, 12747 (2000)]

The heme proximal ligand of carbonmonoxy CooA, a CO-sensing transcriptional activator, in the CO-bound form was identified to be His77 by using picosecond time-resolved resonance Raman spectroscopy. On the basis of the inverse correlation between Fe–CO and C–O stretching frequencies, we proposed previously that His77 is the axial ligand trans to CO (Uchida *et al.*, *J. Biol. Chem.* **273**, 19988), whereas later a possibility of displacement of His77 by CO with retention of another unidentified axial ligand was reported (Vogel *et al.*, *Biochemistry* **38**, 2679). Although our previous resonance Raman study failed to detect the Fe–His stretching [ν(Fe–His)] mode of CO-photodissociated CooA of the carbonmonoxy adduct due to the rapid recombination, application of picosecond time-resolved resonance Raman technique enabled us to observe a new intense line assignable to ν(Fe–His) at 211 cm^{-1} immediately after photolysis, while it became nondiscernible after 100-ps delay. The low ν(Fe–His) frequency of photodissociated CooA indicates the presence of some strain in the Fe–His bond in CO-bound CooA. This and the rapid recombination of CO characterize the heme-pocket of CooA. The 211 cm^{-1} band was completely absent in the spectrum of the CO-photodissociated form of His77-substituted mutant but the Fe-Im stretching band was observed in the presence of exogenous imidazole (Im). Thus, we conclude that His77 is the axial ligand of CO-bound CooA and CO displaces the axial ligand *trans* to His77 with retention of ligated His77 to activate CooA as the transcriptional activator.

II-H-4 A Role of Solvent in Vibrational Energy Relaxation of Metalloporphyrins

MIZUTANI, Yasuhisa; KITAGAWA, Teizo

[*J. Mol. Liq.* in press (2000)]

The formation of a vibrationally excited photoproduct of metalloporphyrins upon (π,π*) excitation and its subsequent vibrational energy relaxation were monitored by picosecond time-resolved resonance Raman spectroscopy. Stokes Raman bands due to a photoproduct of nickel octaethylporphyrin (NiOEP) instantaneously appeared upon the photoexcitation. Their intensities decayed with a time constant of ~300 ps, which indicates electronic relaxation from the (*d*,*d*) excited state (B_{1g}) to the ground state (A_{1g}), being consistent with the results of transient absorption measurements by Holten and coworkers. Anti-Stokes ν_4 and ν_7 bands for vibrationally excited (*d*,*d*) state of NiOEP decayed with time constants of ~10 and ~300 ps. The former is ascribed to vibrational relaxation, while the latter corresponds to the electronic relaxation from the (d,d) excited state to the electronic ground state. While the rise of anti-Stokes ν_4 intensity was instrument-limited, the rise of anti-Stokes ν_7 intensity was delayed by 2.6 ± 0.5 ps, which indicates that intramolecular vibrational energy redistribution has not been completed in subpicosecond time regime. To study a mechanism of intermolecular energy transfer, solvent dependence of the time constants of anti-Stokes kinetics was investigated using various solvents. No significant solvent dependence of the rise and decay constants was observed for NiOEP. For an iron porphyrin, we observed two phases in intermolecular energy transfer. The fast phase was insensitive to solvent and the slow phase depended on solvents. A model of classical thermal diffusion qualitatively reproduced this behavior. For solute-solvent energy transfer process, low-frequency modes of proteins seem to be less important.

II-I Molecular and Electronic Structures of Metallofullerenes and the Fullerene Radical Anions

The continued interest in radical ions of fullerenes and metallofullerenes has resulted from the discovery of superconductivity in the CT complexes of alkali metals with fullerenes. Spectroscopic information concerning the electronic and spin states of the metallofullerenes has been obtained by cw- and pulsed-EPR measurements.

II-I-1 2D-HYSCORE Measurements of ^{13}C–La@C_{82}

OKUBO, Shingo; KATO, Tatsuhisa; AKASAKA, Takeshi[1]; DINSE, K.-P.[2]
([1]Niigata Univ.; [2]TU Darmstadt)

ESEEM (electron spin echo envelope modulation) was detected in the pulsed ESR (Electron Spin Resonance) measurements for two isomers of La@C_{82}. Especially the isomer I of La@C_{82} showed the prominent modulation with the frequency of 3 MHz, which was originated from ^{139}La nuclear quadrupole coupling. The origine of the 3 MHz modulation was confirmed by HYSCORE (Hyperfine Sublevel Correlation Spectroscopy) 2D measurements. ^{139}La quadrupole coupling constant of La@C_{82}-I was directly determined.

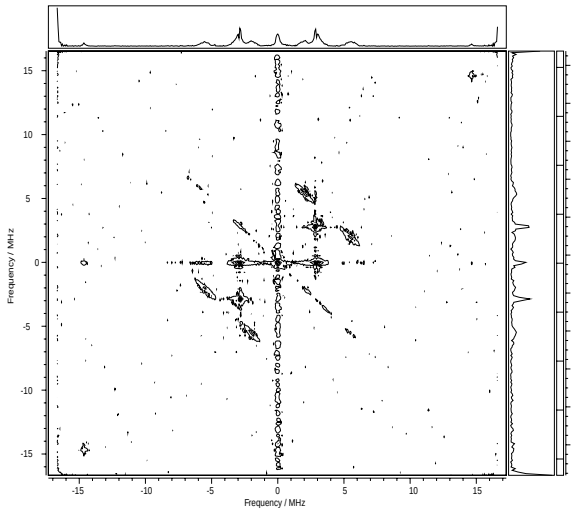

Figure 1. 2D-HYSCORE spectrum of the major isomer of ^{13}C–La@C_{82} obtained at 80 K.

II-I-2 ESR Measurements of La@C_n

OKUBO, Shingo; KATO, Tatsuhisa

Full separation of topological isomers of each La@C_n component (n = 76 to 90) was attempted by 2-stage HPLC separation with chlorobenzene eluent, and all species of La@C_n with even number n from 76 to 90 were detected. Among them La@C_{76}, La@C_{80}-I, II, La@C_{84}-I, and II were newly purified, La@C_{78}, La@C_{86}, and La@C_{88} were partially purified. Their ESR spectra were obtained, as shown in figure, and ESR parameters were determined. Enormous variety of ESR spectra of La@C_ns was obtained in terms of g factor, hyperfine coupling constant, and line width. The topological cage structure of La@C_n reflected on the specific values of the ESR parameter. The anisotropic components of g factor, hyperfine coupling constant, and quadrupole coupling constant were estimated from the temperature dependence of the line width of each La@C_n.

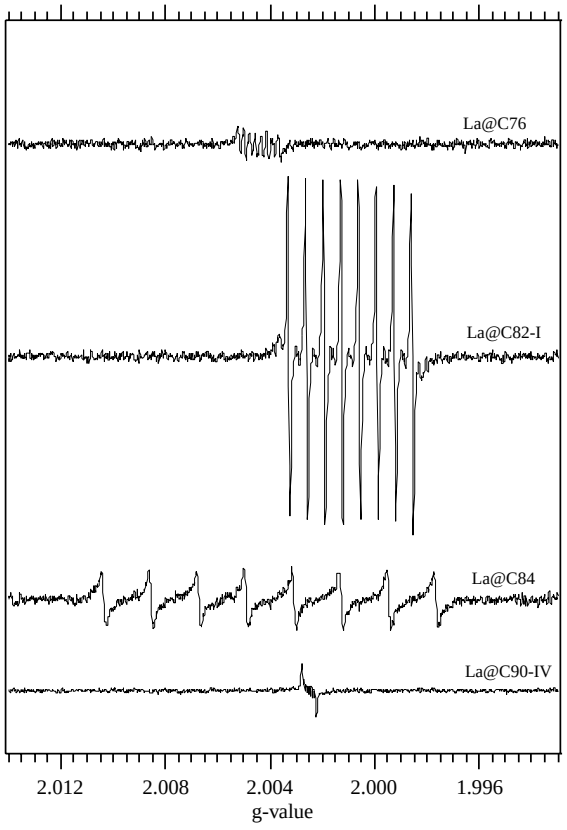

Figure 1. ESR spectra of La@C_{76}, La@C_{82}-I, La@C_{84}, and La@C_{90}-IV measured at room temperature in CS_2 solution.

II-J State Correlated Raman Spectroscopy

The vibrational Raman polarizability tensor responds to molecular reorientational relaxation process, and the structural environment in condensed media. The measurement of Raman scattering is a powerful technique for the study of molecular motion and of the mechanism of phase transition. We've built up the system of multichannel type detection of Raman scattering combined with the temperature controlled cell.

II-J-1 Investigations of Orientational Order for an Antiferroelectric Liquid Crystal by Polarized Raman Scattering Measurements

HAYASHI, Naoki; KATO, Tatsuhisa

The orientational ordering of the antiferroelectric liquid crystal molecules, MHPOBC was investigated in the series of the successive smectic phases by means of polarized Raman scattering measurement without any external field. An improved equation for the analysis of the polarized Raman intensity was derived as a function of an incident laser polarization and the orientational order parameters. Even in the chiral smectic phases, some apparent orientational order parameters could be defined by the proper corrections for the smectic layer structure and an optical disturbance. An unusual change of the orientational order parameters was observed with decrease in temperature. It was concluded that the irregular variation of the order parameter stemmed from the biaxiality of the molecular orientational distribution, which was attributed to the hindrance of molecular rotation around its long axis.

II-J-2 Polarized Raman Scattering Study for Frustoelectric Liquid Crystals

HAYASHI, Naoki; KATO, Tatsuhisa

Orientational ordering for two types of “V-shaped” switching liquid crystals was investigated by polarized Raman scattering measurements. One liquid crystal is based on the ferrielectric phase and the other on the antiferroelectric phase. The apparent orientational order parameters $\langle P_2(\cos\theta)\rangle_{app}$ and $\langle P_4(\cos\theta)\rangle_{app}$ obtained for the ferrielectric based liquid crystal,

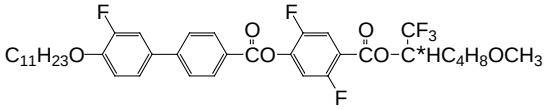

are shown in Figure 1. Square marks show the order parameters obtained with the static electric field of 7 V/μm, circle marks show those without static electric field, and triangle marks show those at the tip of the V-shaped switching. The electric field at the tip of the V-shaped switching is effectively zero, however, the observed order parameters exhibit the similar values of those obtained with the static electric field of 7 V/μm, which are much larger than without static electric field. On the other hand, smaller order parameters were preliminarily obtained at the tip of the V-shaped switching for the other type of antiferroelectric based liquid crystals. The careful comparison of the apparent order parameters for two types of liquid crystal should be necessary for the realistic interpretation of the “V-shaped” switching mechanism.

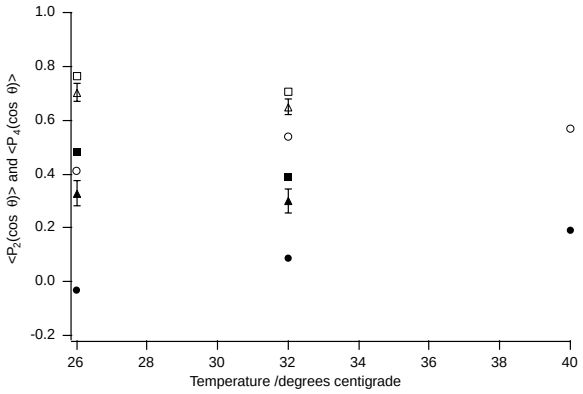

Figure 1. Temperature dependence of apparent orientational order parameters. Open marks show $\langle P_2(\cos\theta)\rangle$ and closed marks show $\langle P_4(\cos\theta)\rangle_{app}$. Square; with the static electric field of 7 V/μm, circle; without static electric field, triangle; at the tip of the V-shaped switching.